ULTRAFAST CHARGING COMPATIBILITY OF ELECTRIC VEHICLES

M. Tsirinomeny, H. Hõimoja, A. Rufer

EPFL - Swiss Federal Institute of Technology Lausanne, Lausanne, Switzerland

Abstract
To increase the appeal of electric vehicles, the trend is to shorten the charging time and to lengthen the autonomy. The new ultrafast charge compatible battery on lithium-titanate gives the best compromise between high power and energy densities. The main objective of the contribution is to demonstrate the state-of-the-art of the fast charged electric vehicles and propose an evaluation tool for determining the possibility of shortened charging times from the traction battery viewpoint.

Introduction
An evident nuisance for electric vehicle (EV) owners is the limited average speed while driving long distances on highways, as recharging stops, defined by the battery performance, lengthen the total travelling time. Moreover, in the framework of on-board energy storage, one of the main problems is that the charge and discharge processes of a battery are asymmetrical in time, meaning that a sustainable recharge takes usually much more time than discharge[1]. Therefore, substantial progress can be expected in the area of on-board energy storage technologies; this paper shows the compatibility of ultra-fast battery for the existing EV.

As for today, the commercially available solutions allow recharging of an EV within 20 min as minimum[2,3]. High energy density lithium batteries, based mostly on the lithium-manganese spinel (LMO) or lithium-iron phosphate (LFP) electrochemistries are widely used by manufactures in order to reach the highest autonomy possible with a disadvantage long charging time in scale of 6 h from a conventional household socket. Whereas high power density batteries require less time to recharge, their energy density and autonomy show poorer figures. A qualitative comparison between available EV battery chemistries is shown in Fig. 1. It should pointed out, however, that the manufacturers often specify the specific power as absolute maximum during a 10 s pulse, therefore the datasheet values should be interpreted with reservation unless there are more detailed figures available, not to mention different specific power for charging and discharging.

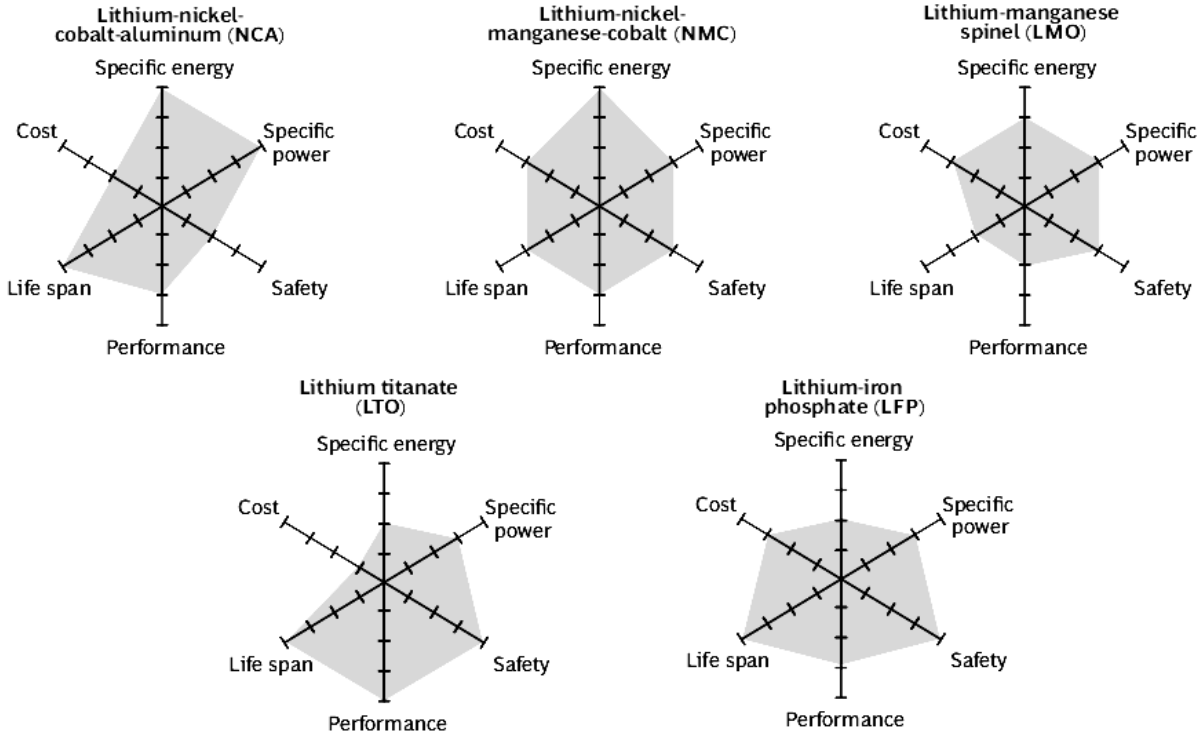

Fig. 1. A comparison between main lithium ion battery chemistries[4]

The Fig. 1 together with additional market research permits concluding that the optimal EV battery electrochemistry in terms of recharge-discharge symmetry, life span, specific power and energy is that of the lithium titanate (LTO, or chemically expressed $Li_4Ti_5O_{12}$)[5]. However, a trade-off between charging power density and specific energy exist, meaning an EV must be recharged more frequently than by using existing battery though the average speed is improved (Fig. 2). A nearly similar approach has been recently applied in refilling compressed air propelled vehicles[6]

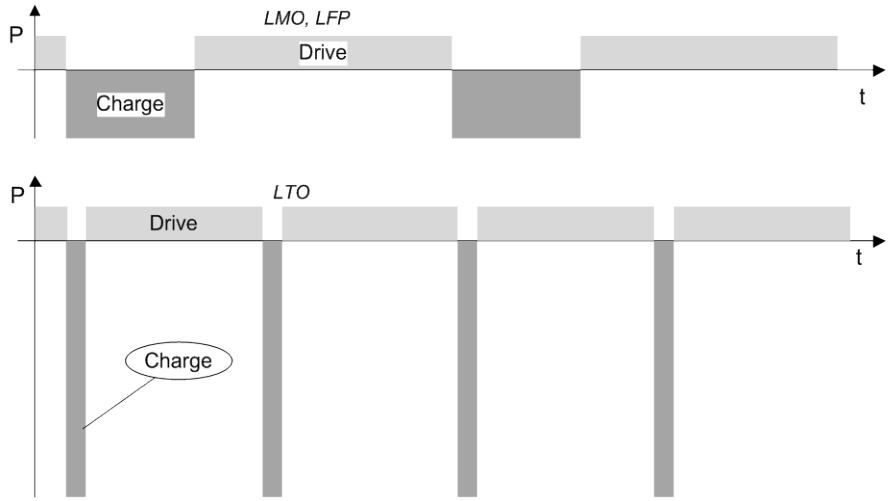

Fig. 2. Charging-driving ratio at existing and proposed battery electrochemistries

Materials and Methods

The design of an EV ultrafast charging compatibility evaluation tool starts with creating a generic EV model, composed of the main battery and traction subsystem (Fig. 3). In the battery subsystem, the cell modules supply the vehicle with electric energy through the dc bus. A standard half- bridge dc/dc chopper is used to adapt the variable voltage from the battery to the quasi-constant voltage in the dc bus. Braking energy is partially recovered during deceleration. The traction subsystem is composed of an electric machine and a full bridge voltage source inverter (VSI). Transmission gear is used to adapt the speed ratio between wheels and the motor shaft, followed by a mechanical differential changing the speed ratio between the two traction wheels.

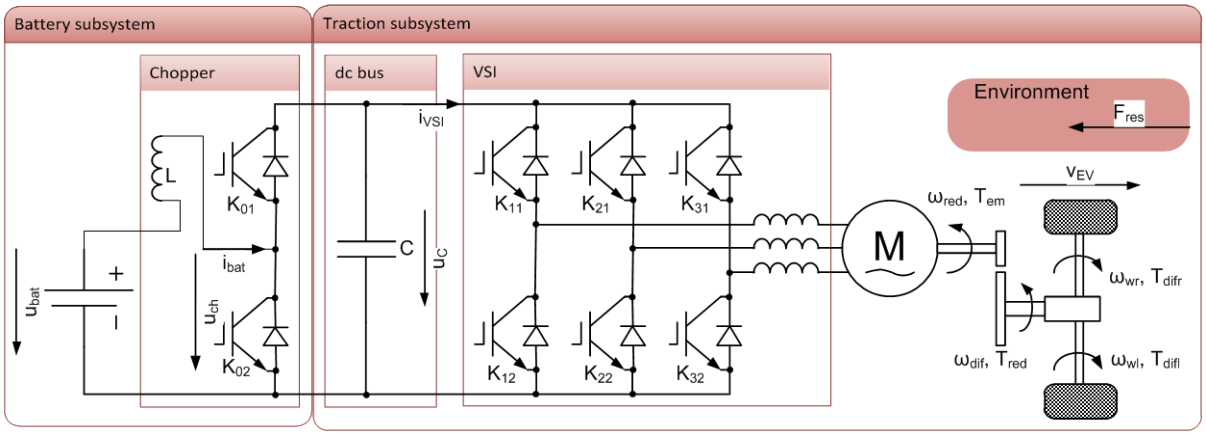

Fig. 3. Studied EV model

The movement of an EV is simulated during the New European Driving Cycle (NEDC), which reflects both urban and extra-urban driving conditions and is set as standard to characterise the energy consumption of small vehicles. The simulation model helps to validate the battery's ability to supply sufficient power to follow the NEDC load curve.

The performance of the upgraded EV is modelled using the Energetic Macroscopic Representation (EMR). EMR is a graphical description, which organises the system into interconnected basic subsystems: accumulators, sources, conversion and distribution. All elements are connected according to the interaction principle. The product of the action (for example, the force) and reaction

(for example, the velocity) always leads to the power exchanged by the connected elements. Moreover, all elements are described using the physical causality (i.e. integral causality). These properties enable a systematic deduction of the control scheme[7].

In the first step, the EV main battery is considered as an equivalent electric source, where the voltage as state variable is derived from the current. The LTO has been modelled by its nonlinear open circuit voltage (OCV) connected in serial with two parallel resistances representing the internal resistance values for charge and discharge (Fig. 4).

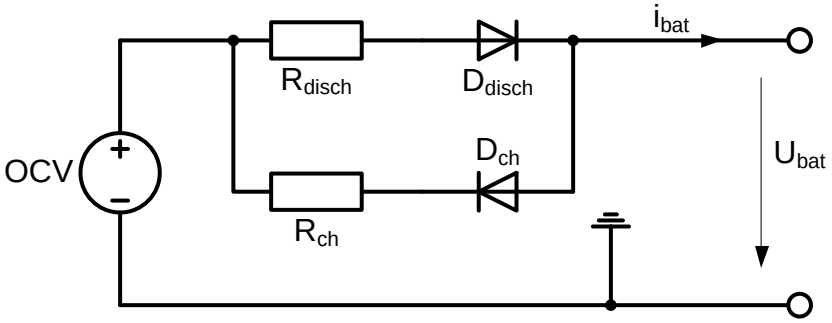

Fig. 4. LTO battery equivalent schema

The battery state of charge (*SoC*) has a strong relation with coulomb (ampere-hour) capacity Q_{bat}, charge or discharge current and the previous state of charge:

$$SoC(t+1) = SoC(t) + \int_0^{t+1} \frac{i_L}{Q_{Bat}} dt = SoC(t) + \frac{\Delta t}{Q_{Bat}} \sum_{i=t}^{t+1} i_{L,\Delta t} \tag{1}$$

The chopper is represented as an electric conversion element. The dc bus is represented by a capacitor as energy accumulation element with voltage u_C as the state variable.

$$C \frac{d}{dt} u_C = i_{bat} - i_{VSI} \tag{2}$$

The chopper inductance L is represented by an accumulation element with the current i_{bat} as action variable. This current depends on the battery pack voltage u_{bat}, chopper voltage u_{ch} and internal resistance r_{bat}.

$$L \cdot \frac{d}{dt} i_{bat} + r_{bat} \cdot i_{bat} = u_{ch} - u_{bat} \tag{3}$$

For electromechanic conversion, a permanent magnet synchronous machine (PMSM) is chosen because thanks to enhanced power density and ample use in EV design.

$$i_{VSI} = \frac{T_{em}\omega_{red} - P_{loss}}{u_C} = \frac{T_{em}\omega_{red}}{u_C} - \eta_{em} i_{VSI} \tag{4}$$

In (4), T_{em} stands for electromechanical torque at the motor shaft, ω_{red} for the input angular speed on the reduction gear, P_{loss} for the power loss and η_{em} for the electromechanic conversion efficiency. The latter value is not constant, but depends on the actual motor operating point. In Fig. 5, the motor efficiency map for Toyota Prius is shown, the values scaled for further modelling to match actual drivetrain power.

Reduction gear is represented by a mechanical conversion element with transmission ratio k_{red} and efficiency η_{red}.

$$\begin{cases} T_{red} = \eta_{red} \cdot k_{red} \cdot T_{em} \\ \omega_{red} = k_{red} \cdot \omega_{diff} \end{cases} \tag{5}$$

Differential is represented by a mechanical coupling element with transmission ratio k_{dif} and efficiency η_{dif}, enabling the left and right wheel to spin at different angular speeds ω_{wl} and ω_{wr}, respectively.

$$\begin{cases} T_{dif} = \eta_{dif} \cdot k_{dif} \cdot T_{red} \\ \omega_{dif} = k_{dif} \cdot (\omega_{wl} + \omega_{wr}) \end{cases} \tag{6}$$

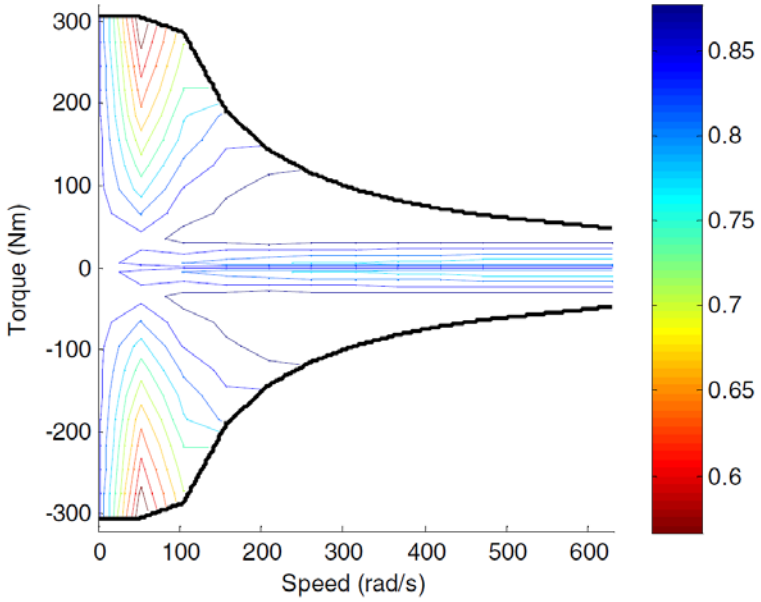

Fig. 5. A 30 kW PMSM efficiency map for Toyota Prius[8]

The wheels are represented by a mechanical conversion element with radius R_w:

$$\begin{cases} F_{wl} = \dfrac{1}{R_w} T_{difl} \\ F_{wr} = \dfrac{1}{R_w} T_{difr} \end{cases} \tag{7}$$

$$\begin{cases} \omega_{wl} = \dfrac{1}{R_w} v_l \\ \omega_{wr} = \dfrac{1}{R_w} v_r \end{cases} \tag{8}$$

$$\begin{cases} F_{wl} + F_{wr} = F_{tot} \\ v_l + v_r = v \end{cases} \tag{9}$$

The chassis is represented by an accumulation element with the velocity of electric vehicle v as the objective state variable. The equivalent mass of the vehicle m_{eq} comprises, besides the actual mass m_{EV}, the inertia of rotating parts, expressed by additional inertia percentage γ = 2 %...5 % for road vehicles.

$$\begin{cases} m_{eq} \cdot \dfrac{d}{dt} v = F_{tot} - F_{res} \\ m_{eq} = m_{EV} \cdot (1+\gamma) \end{cases} \tag{10}$$

The resistive force F_{res} posed by the environment, is a sum of three basic components:

1) rolling resistance, determined by vehicle's mass and tyre friction;
2) aerodynamic resistance, determined by vehicle's geometry and velocity squared;
3) slope resistance, determined by the vehicle's mass and slope angle.

The difference between total force F_{tot} delivered by the drivetrain and three-component resistive force F_{res} builds up the so-called dynamic force, accelerating or decelerating the vehicle in dependence of the sign.
Finally, inversion based control is deduced from inversion of EMR. PI controllers are used to control the objective velocity and dc bus voltage (Fig. 6).

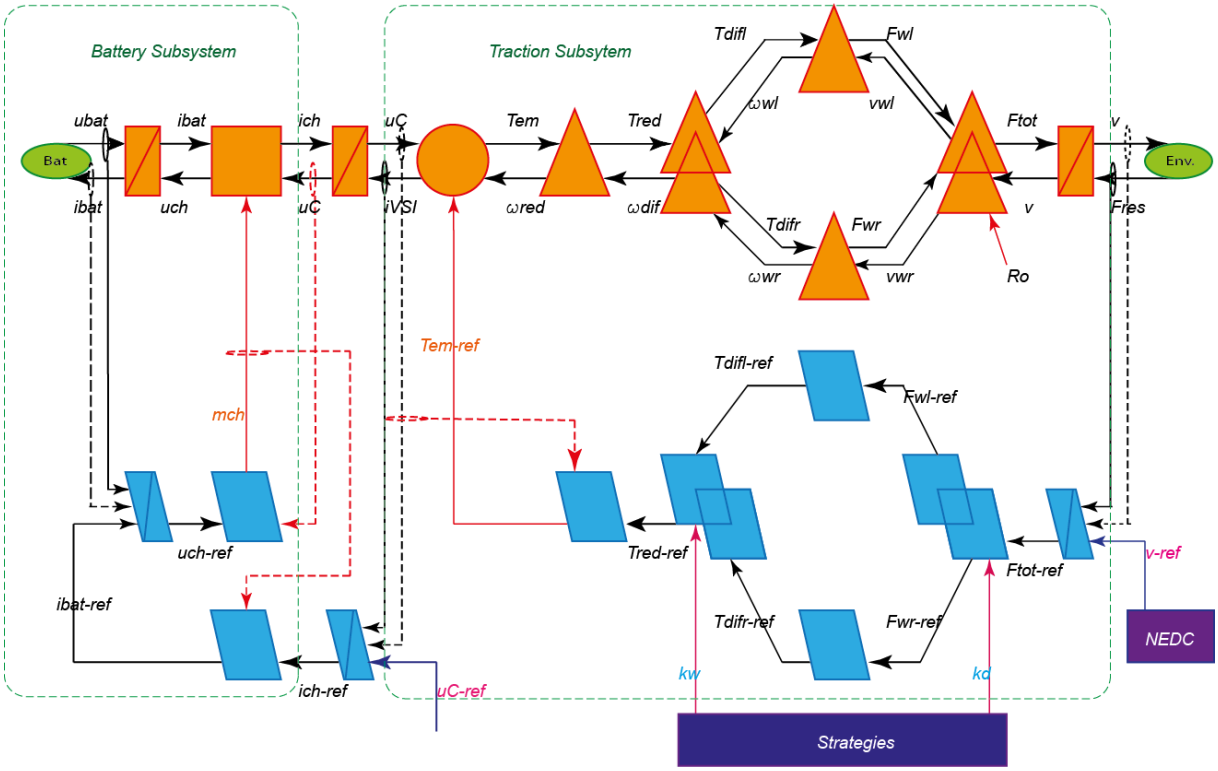

Fig. 6. EV model, based on the energetic macroscopic representation

Results and Discussion

For the simulations, 16 kW·h LTO battery pack is used with estimated mass of 390 kg in comparison to original iMiEV 250kg. The specific power of the PMSM is estimated 2.2 kg/ kW. Therefore, the total estimated mass of EV with 3 passengers is 1450 kg.

In Fig. 7, vehicle simulation results with state-of-the-art “quick” charging are shown. Here, the charging current is numerically equal to twofold coulomb capacity. The initial *SoC* of the battery is taken equal to 80 %, which is a usual upper limit with constant current charging. During a 1200 s (20 min) cycle, approximately 0.75 kW·h is withdrawn from the main battery. The negative power values reflect regenerative braking, which is limited by the EV drivetrain and the battery itself. The poor tank-to-wheel (TTW) efficiency can be explained both by the motor performance (Fig. 5) and the losses inside the battery itself.

Under ultrafast charging conditions, the charging current equals tenfold coulomb capacity. The LTO batter can more effectively absorb regenerative braking energy, thus improving overall TTW efficiency and reducing energy consumption per distance travelled (0.5 kW·h), meaning a battery with same capacity can provide more autonomy.

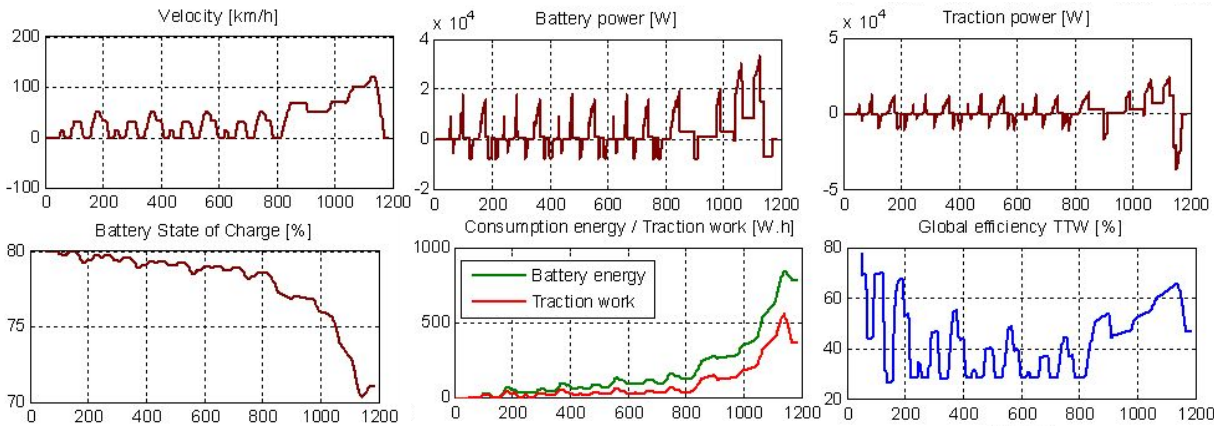

Fig. 7. Simulation results with “quick” charging

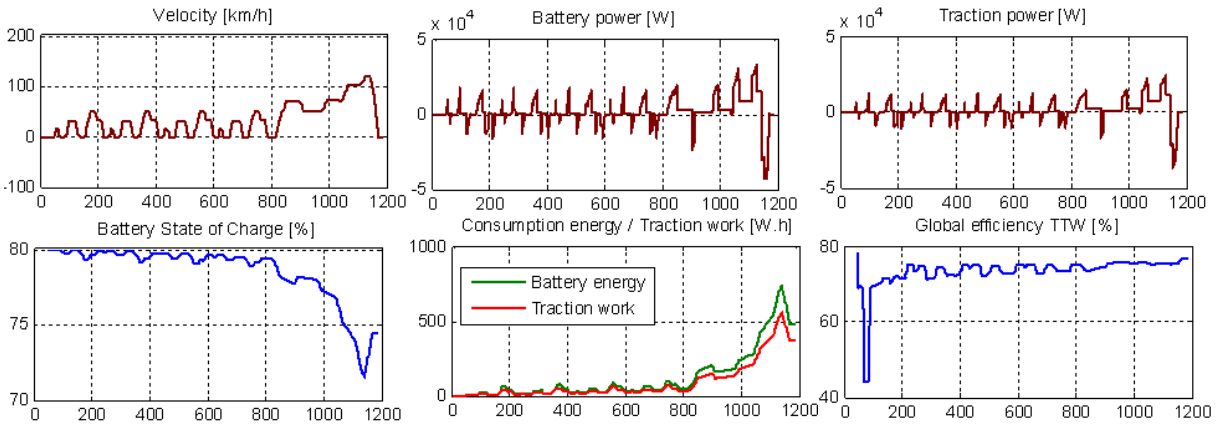

Fig. 8. Simulation results with ultrafast charging

For final conclusions, one of the advantages of an ultrafast charge compliant EV battery such as LTO is that it can absorb more regenerative energy in comparison with other chemistries. Therefore, in urban conditions, the range of the electric vehicle increases at the same battery capacity. A LTO battery pack weighing in the range of 390 kg can yield autonomy of 210 km in comparison to a default iMiEV battery with 250 kg mass and 150 km NEDC range[2]. In contrast, the major drawback of ultrafast charge compliant battery is its quite low energy density, minimising the vehicle range during the extra-urban driving conditions at the same mass and volume. However, the simulation shows that the global efficiency is still bad, because the electric machine works in its suboptimal window. Therefore an automatic transmission such as direct shift gearbox (DSG) is recommended in order to reach always the maximum power point tracking (MPPT). Next step in the research is to achieve experimental results in order to validate the initial modelling and calculation ones.

Acknowledgements

The authors would like to thank The Competence Centre Energy and Mobility (CCEM) as well as the Swisselectric Research for their continuous support to the EPFL industrial electronics laboratory research team in the field of EV infrastructure related studies.

References

[1] K. Zaghib, J.B. Goodenough, A. Mauger, C. Julien. Unsupported claims of ultrafast charging of LiFePO4 Li-ion batteries. Journal of Power Sources, No. 194, 2009, pp. 1021-1023.

[2] Observatoire du Véhicule d'Entreprise: http://www.observatoire-vehicule-enterprise.com/

[3] M. Kamachi, H. Miyamoto, Y. Sano. Development of Power Management System for Electric Vehicle "i-MiEV", International Power Electronics Conference, 2010, pp. 2949-2955.

[4] The Boston Consulting Group. Batteries for Electric Cars. Challenges, Opportunities, and the Outlook to 2010. Available online: http://www.bcg.com/documents/file36615.pdf, 18 pages.

[5] The Altairnano Company : http://www.altairnano.com/

[6] A. Rufer, S. Lemofouet, M. Habisreutinger, M. Heidari, A. Leuba. Driving and Filling Personal Vehicles – The Questions of Energy - and Power - Density (A Fast Filling Station for the Compressed Air Car), 2011 Geneva World Engineers' Convention, 9 p.

[7] W. Lhomme, P. Delarue, A. Bouscayrol., P. Le Moigne, A. Rufer. Comparison of Control Strategies for Maximizing Energy in a Supercapacitor Storage Subsystem. EPE Journal Vol. 19, No. 3, September 2009, pp. 5-14.

[8] J. Poxon, A. McGordon, G. Muraleedharakurup, P. Jennings. Determining a suitable all electric range for a light weight plug-in hybrid electric vehicle. IEEE Vehicle Power and Propulsion Conference (VPPC), 2010, pp. 1-8.